Bima Journal of Science and Technology, Vol. 8(4A) Dec, 2024 ISSN: 2536-6041

DOI: 10.56892/bima.v8i4.1152

# Geochemical Characterization of Baryte Mineralization in the Gombe Inlier, Gongola Sub-basin, Northern Benue Trough, Nigeria: Insights into Its Origin and Physico-Chemical Conditions

Auwalu Dalha[1]*, Ahmed Isah Haruna[2] and Abubakar S. Maigari[2]

[1]Department of Geology, Gombe State University, P.M.B.0127, Gombe, Nigeria
[2]Department of Applied Geology, Faculty of Science, Abubakar Tafawa Balewa University, P.M.B. 0248, Bauchi, Nigeria
Corresponding Author: dalhaauwalu1057@gmail.com

## ABSTRACT

A detailed investigation was conducted on a baryte mineralization located in the Gombe Inlier within the Gongola Sub-basin of the Northern Benue Trough. The study aimed to determine the physico-chemical conditions of baryte crystallization and to gain insights into the ore genesis of the baryte mineralization in the Gombe Inlier through geochemical analysis. Using a Rigaku NEX DE X-ray fluorescence (EDXRF) spectrometer, we measured both the major and trace elements, as well as rare earth elements, present in the baryte ores. Geochemical investigations indicated that the baryte veins contain an average concentration of 72.86 wt.% BaO and 2.10 wt.% SrO. The mineralizing fluid is characterized as a strongly differentiated hydrothermal fluid, rich in Ba and Sr while being poor in high field strength elements (Hf, Zr, Ta, Nb, and rare earth elements), which precipitated earlier. Late-stage fluids typically concentrate incompatible elements like Ba and Sr, suggesting that the baryte deposits in the Gombe Inlier are part of the baryte end-member of the baryte-celestine solid solution series. The Ba-rich fluids are derived from magmatic hydrothermal fluids (juvenile water) and the leaching of oceanic or continental rocks, or a combination of both. The presence of Cu, Pb, Zn, and Fe oxides (in form of hematite), along with fluctuations in the Eu anomaly in both baryte fields, further supports the precipitation of baryte minerals by seawater-bearing hydrothermal fluids in fluctuating oxic-anoxic conditions within a low-temperature or near-surface environment. Variations in elevation from the Southern to the Northern Benue Trough contributed to changes in the redox conditions affecting baryte mineralization throughout the Benue Trough.

**Keywords:** Gombe inlier, Benue Trough, geochemistry, baryte, genesis

## INTRODUCTION

Minerals in the baryte ($BaSO_4$) solid solution series are found in a wide variety of sedimentary, metamorphic, and igneous environments, spanning from the Early Archean (~3.5 Ga) to the present (Honor, 2000). Most baryte in the Earth's crust has formed through the mixing of two fluids; one containing Ba leached from silicate minerals and the other an oxidized, shallow fluid like seawater that contains sulfate. Large baryte deposits mark zones of concentrated fluid flow and mineral precipitation, helping to reconstruct the Earth's hydrogeologic history. Since baryte's stability is redox-sensitive, its presence or absence provides key insights into paleoredox conditions of some mineral's crystallization. Therefore, the geochemical composition of baryte reflects the regional mineralization and the physicochemical conditions under which it crystallized (Jamieson et al., 2016).

Most major baryte deposits have formed in tectonic settings where deep waters carrying Ba and Sr rich metals rise into shallow, oxidizing environments where sulfate is stable.

DOI: 10.56892/bima.v8i4.1152

Fluids in sedimentary basins and continental crust are influenced by forces like topography-driven flow, free convection, and forced convection, which can cause large-scale fluid migration (Cathles, 1997; Garven & Raffensperger, 1997). In oceanic crust, fluid flow is mainly driven by thermal convection from magmatic heat. Extensional faulting is key to localizing many baryte deposits, which can form in diverse tectonic settings such as compressional margins, rift basins, passive margins, and oceanic crust (Cathles, 1997).

The Gombe Inlier is a significant geological feature in northeastern Nigeria, showcasing the Cretaceous geology of the Northern Benue Trough through well-exposed, easily accessible outcrops. It is located within the Gongola sub-basin, a north-south trending arm of the Benue Trough, and is separated from the east-west trending Yola Arm by an area of shallow Basement rocks known as the "Wuyo-Kaltungo High" (Zaborski, 1998; 2003). Baryte, along with other minerals such as fluorite and chalcopyrite, has been reported in the Gombe Inlier. These minerals are primarily hosted in Basement and sedimentary rocks, mainly gneiss, silcretes and Bima sandstones (Figure 1b). Detailed studies on the occurrences and structural features hosting the mineralization can be found in the works of Auwalu et al. (2024), Rabiu et al. (2019), MMSD (2010), and Haruna (2007). Most research in this area focuses on the structural settings of the mineralization and the exposed stratigraphic sequence along the inlier's flanks (Auwalu et al., 2024; Rabiu et al., 2019; Byemi et al., 2015; Haruna, 2007; Zaborski, 1998). Despite previous studies in the Gombe Inlier, there has been a lack of critical information regarding the chemistry of baryte mineralization and its associated minerals, as well as an understanding of the economic implications of this mineralization and the relationships among the minerals. Currently, only unregistered miners exploit baryte in the Gombe Inlier, making the economic impact of this mineralization nearly impossible to assess. This study aims to utilize geochemical data from baryte ore minerals to elucidate the physico-chemical conditions of baryte crystallization and to provide insights into the ore genesis of baryte mineralization in the Gombe Inlier.

## GEOLOGICAL SETTINGS

The Benue Trough in Nigeria is a rift basin approximately 1,000 km long and 250 km wide, with Cretaceous–Tertiary sediments that can reach depths of up to 6,000 m. Sediments older than the Mid-Santonian have experienced compression, folding, faulting, and uplift in various areas. The Mid-Santonian tectonic episode caused significant compressional folding, resulting in over 100 anticlines and synclines within the Trough (Benkhelil, 1989). The origin of the Benue Trough is closely linked to the Early Cretaceous opening of the Atlantic Ocean, and several models have been proposed to explain its formation (Stoneley, 1966; Grant, 1971; Olade, 1975; Benkhelil, 1989; Guiraud and Maurin, 1992).

The Benue Trough is geographically divided into three sub-basins: Lower, Middle, and Upper Benue Trough. These segments are further classified into Southern (Lower), Central (Middle), and Northern (Upper) sections (Nwajide, 2013). The Northern Benue Trough includes the Yola and Gongola sub-basins, where Cretaceous sediments overlay the Precambrian Basement Complex (Figure 2).

DOI: 10.56892/bima.v8i4.1152

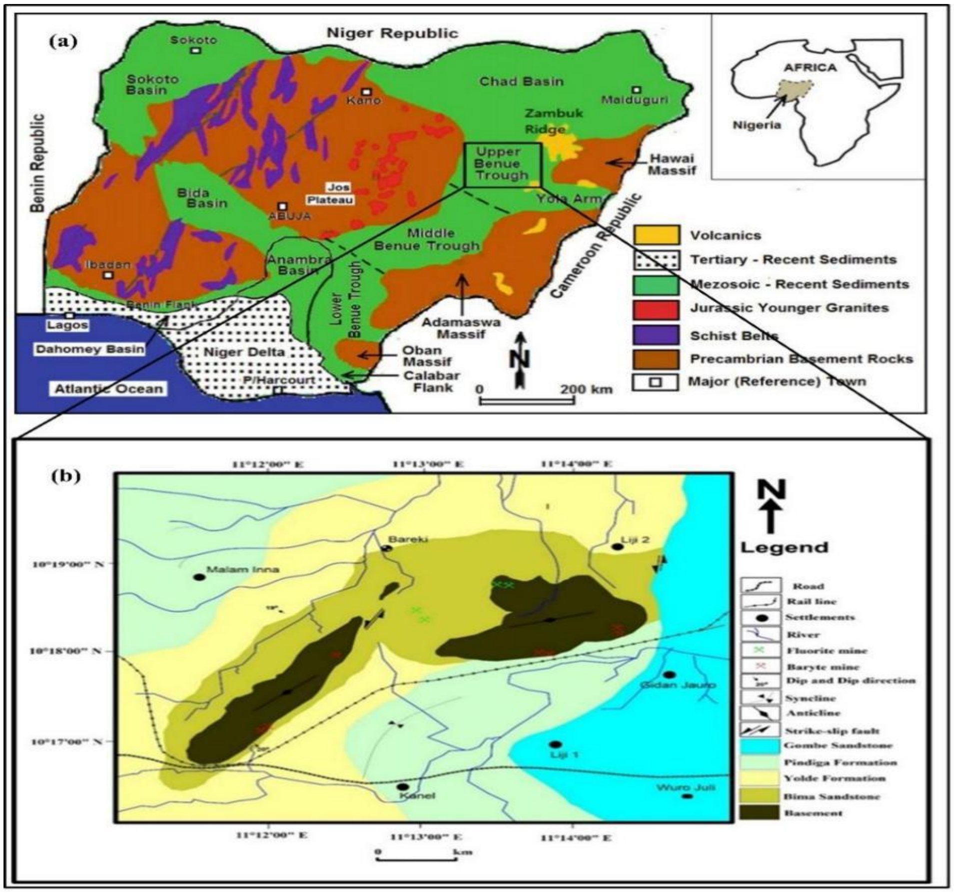

**Figure 1:** **(a)** Location and geological setting of the Benue Trough, Nigeria modified after Tijani and Loehnert, (2004), **(b)** Geological map of the study area (Auwalu et al., 2024).

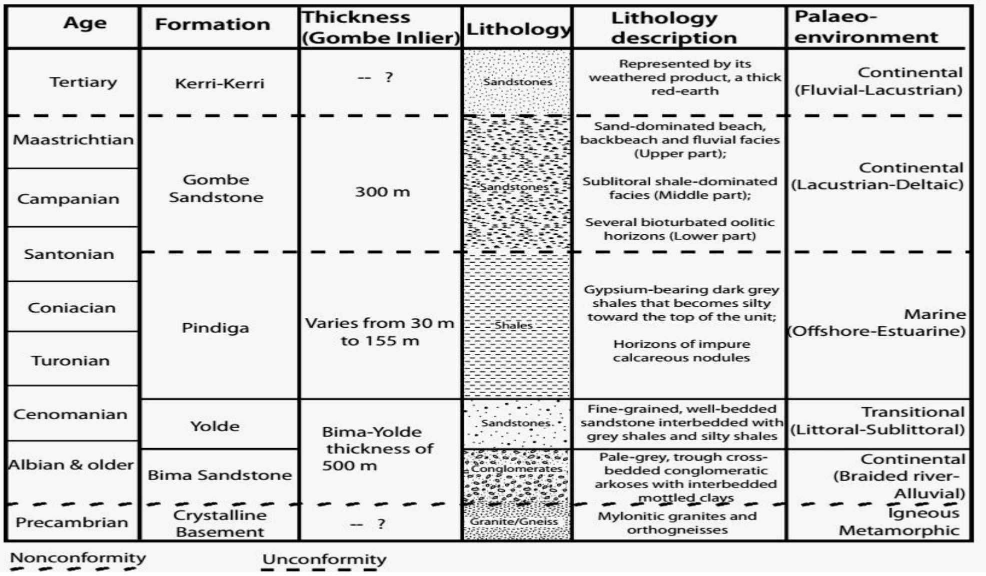

| Age | Formation | Thickness (Gombe Inlier) | Lithology | Lithology description | Palaeo-environment |
|---|---|---|---|---|---|
| Tertiary | Kerri-Kerri | -- ? | Sandstones | Represented by its weathered product, a thick red-earth | Continental (Fluvial-Lacustrian) |
| Maastrichtian | Gombe Sandstone | 300 m | Sandstones | Sand-dominated beach, backbeach and fluvial facies (Upper part);<br>Sublitoral shale-dominated facies (Middle part);<br>Several bioturbated oolitic horizons (Lower part) | Continental (Lacustrian-Deltaic) |
| Campanian | | | | | |
| Santonian | | | | | |
| Coniacian | Pindiga | Varies from 30 m to 155 m | Shales | Gypsium-bearing dark grey shales that becomes silty toward the top of the unit;<br>Horizons of impure calcareous nodules | Marine (Offshore-Estuarine) |
| Turonian | | | | | |
| Cenomanian | Yolde | Bima-Yolde thickness of 500 m | Sandstones | Fine-grained, well-bedded sandstone interbedded with grey shales and silty shales | Transitional (Littoral-Sublittoral) |
| Albian & older | Bima Sandstone | | Conglomerates | Pale-grey, trough cross-bedded conglomeratic arkoses with interbedded mottled clays | Continental (Braided river-Alluvial) |
| Precambrian | Crystalline Basement | -- ? | Granite/Gneiss | Mylonitic granites and orthogneisses | Igneous Metamorphic |

Nonconformity
Unconformity

**Figure 2:** Stratigraphic succession of Gongola Sub-Basin of the Northern Benue Trough (Byemi et al., 2015).

DOI: 10.56892/bima.v8i4.1152

The oldest sedimentary rocks in the Gongola Sub-basin of the Northern Benue Trough are the Bima sandstones, which are unconformably positioned above the Mylonitic Granites and Orthogneisses of the Basement complex (Figure 2). The Bima Group, comprising lower, middle, and upper Bima Sandstones, is the most extensive sedimentary sequence in the Northern Benue Trough, with thicknesses reaching up to 1,500 m (Zaborski, 2003; Zaborski et al., 1998). These sandstones, representing the characteristic of an active rift stage in basin development and exhibit pale-grey, trough cross-bedded conglomeratic arkoses, often mixed with purple mottled clays. This Formation is indicative of an alluvial fan braided river deposit (Guiraud, 1990a).

The Yolde Formation was formed during a transitional period as the environment shifted from the primarily continental conditions of the early Cretaceous to the predominantly marine conditions of the late Cretaceous (Zaborski, 2003). This Formation consists of fine-grained, well-bedded sandstones and braided-river sediments that resemble those found in the Bima Sandstone. Bioturbation is occasionally observed within the sandstone layers. Furthermore, intercalated clay layers often display pedogenetic characteristics, which can complicate the identification of the Yolde and Bima Sandstones in field observations (Zaborski, 1998, 2003).

The Pindiga Formation primarily consists of shale, characterized by dark grey, gypsum-bearing shales that transition to a silty texture in the upper section of the unit (Figure 2). Within these shales, layers of yellow-grey impure calcareous nodules, commonly referred to as "limestone nodules," are present. These nodules suggest that genuine marine conditions prevailed from the Late Cenomanian to the Mid Santonian period (Zaborski et al., 1998). The Gombe Sandstone was deposited between the Mid Santonian and the end of the Cretaceous period (Maastrichtian) and is distinctly separated from the Pindiga Formation by a significant angular unconformity, which resulted from Mid-Santonian compression (Guiraud, 1993). The base of the Gombe Sandstone features several bioturbated oolitic ironstone horizons, which quickly transition into sublittoral shale-dominated facies in the middle of the unit. Higher in the sequence, the formation consists mainly of sand-dominated beach, back-beach, and fluvial facies, indicating a shift back to continental conditions (Zaborski, 1998, 2003). During the terminal Cretaceous period, a compressional event impacted the Northern Benue Trough, leading to the uplift, faulting, and erosion of the Gombe Sandstone (Zaborski, 1998, 2003).

## MATERIALS AND METHODS

Eighteen (18) baryte samples were pulverized into powder, with approximately 5 grams of each sample placed into 32 mm sample cups lined with 4 µm thick polypropylene X-ray film and hydraulically pressed. The height of the samples was measured, and the sample cups were capped. The major oxides and trace elements were analyzed using a Rigaku NEX DE X-ray fluorescence (EDXRF) spectrometer, which features a fifteen-place sample changer operating in slow, steady spinning mode at the geochemistry laboratory in the Department of Geology at Gombe State University, Nigeria.

EDXRF measurements were conducted in a helium (He) atmosphere using a palladium (Pd) X-ray tube set at 60 kV and 10 µA, with a 10 mm beam spot size and a silicon (Si) drift detector. Elemental quantification of unknown samples was performed using standardless calibration through the Fundamental Parameters (FP) method, facilitated by the Rigaku RPF-SQX software. This software automatically calculates the concentrations of major oxides and trace elements in the baryte samples while applying necessary corrections.

DOI: 10.56892/bima.v8i4.1152

The analytical uncertainties for the Rigaku NEX DE EDXRF typically ranged from 0.1% to 1% (RSD). Detailed descriptions of the Rigaku NEX DE EDXRF spectrometry analysis using the standardless calibration with the FP method can be found in the works of Rousseau (2013) and Croffie et al. (2020).

Data analysis utilized geochemical modeling packages and involved constructing multi-element diagrams with statistical and geo-analytical software, including Microsoft Excel, Geochemical Data Tool Kit (GCDKit), Petrograph, and Surfer 13. The results were presented in the form of tables, figures, and plates, and were interpreted using geological knowledge and additional reference materials.

## RESULTS

Geochemical analysis of the Major, trace and rare earth elements (REE) is a powerful instrument for hydrothermal mineralization studies, and is used in order to recognize the formation and to detect the source of mineralized fluids in different geological environments (see, among others, Guichard et al., 1979; Jewell & Stallard, 1991; Bozkaya & Gökce, 2004; Clark et al., 2004; Jurkovic et al., 2010; Noguchi et al., 2011). Geochemical indicators of baryte mineralization can be obtained through the detection of ore chemistry, as this may help to reconstruct the physio-chemical conditions during precipitation. Two different barytes fields were characterized in Gombe inlier, namely Gombe baryte fields and Liji baryte fields.

### Major Elements

Geochemical concentrations of the major element oxides of baryte separate from Gombe and Liji baryte fields in Gombe Inlier are shown in Table 1. The concentration of $SiO_2$ ranges from 3.50 to 14.3 wt. % (avg. 6.57 wt. %), $Al_2O_3$ ranges from <0.01- 1.42 wt. % (avg. 0.44 wt. %), CaO ranges from 0.031- 18.30 wt. % (avg. 4.95 wt. %), $Fe_2O_3$ ranges from 0.017- 9.83 wt. % (avg. 0.96 wt. %) and $P_2O_5$ ranges from 0.826 1.050 wt. % (avg. 0.90 wt. %) (Table 1). $Na_2O$, $K_2O$, $TiO_2$, MgO and MnO are present with average values of less than 0.01. The concentration of BaO and SrO in the baryte veins ranges from 51.3 – 78.7 wt. % (avg. 72.86 wt. %) and 1.41 – 2.89 wt. % (avg. 2.10 wt. %) respectively (Table 1).

### Trace elements

The trace element composition of baryte from the Gombe and Liji fields is presented in Table 2. When normalized to the average lower continental crust (LCC) values of Taylor and McLennan (1995), the trace element concentrations in baryte samples from both fields show similar distribution patterns, suggesting a genetic relationship between the baryte deposits in Gombe and Liji baryte fields (Figure 3). The baryte samples are notably enriched in Ba, Sr, Nd, and Tb, while being low in high field strength elements such as Hf, Zr, Ta, Nb, and rare earth elements (REEs) compared to background concentrations in barren rocks. This enrichment of Ba and Sr in all baryte samples indicates that the deposits in the Gombe and Liji fields belong to the baryte end-member of the baryte-celestine solid solution series.

DOI: 10.56892/bima.v8i4.1152

**Table 1: Major oxides concentration of mineralized baryte veins from the area of study (all values are in wt. %).**

| Oxides | Baryte separate | | | | | | | | | | | | | | | | | | |
|---|---|---|---|---|---|---|---|---|---|---|---|---|---|---|---|---|---|---|---|
| | Gombe Baryte | | | | | | | | | | | Liji Baryte | | | | | | | |
| | SB1 | SB2 | SB3 | SB4 | SB5 | SB6 | SB7 | SB8 | SB9 | SB10 | SB11 | SB12 | SB13 | SB14 | SB15 | SB16 | SB17 | SB18 | Avg. |
| BaO | 51.30 | 59.90 | 73.50 | 75.80 | 77.00 | 71.20 | 74.00 | 75.50 | 78.00 | 74.30 | 74.60 | 74.20 | 76.70 | 72.80 | 77.00 | 78.70 | 74.00 | 73.00 | 72.86 |
| SrO | 1.41 | 1.77 | 2.33 | 2.70 | 2.51 | 1.87 | 1.78 | 1.59 | 1.59 | 2.04 | 2.17 | 2.12 | 1.70 | 1.86 | 2.86 | 2.89 | 2.11 | 2.46 | 2.10 |
| $SiO_2$ | 14.3 | 8.19 | 5.92 | 6.79 | 4.68 | 9.94 | 5.89 | 7.13 | 6.03 | 4.75 | 4.18 | 4.26 | 8.33 | 6.15 | 4.83 | 3.50 | 9.04 | 4.10 | 6.57 |
| $Al_2O_3$ | 1.42 | 0.54 | <0.01 | <0.01 | 0.91 | 1.10 | 0.61 | 0.93 | 0.62 | 0.80 | <0.01 | <0.01 | <0.01 | <0.01 | <0.01 | <0.01 | 0.92 | <0.01 | 0.44 |
| MgO | <0.01 | <0.01 | <0.01 | <0.01 | <0.01 | <0.01 | <0.01 | <0.01 | <0.01 | <0.01 | <0.01 | <0.01 | <0.01 | <0.01 | <0.01 | <0.01 | <0.01 | <0.01 | <0.01 |
| $Fe_2O_3$ | 9.83 | 0.97 | 0.62 | 1.02 | 2.25 | 0.36 | 0.09 | 0.16 | 0.02 | 0.68 | 0.07 | 0.14 | 0.58 | 0.07 | 0.07 | 0.02 | 0.30 | 0.08 | 0.96 |
| MnO | <0.01 | <0.01 | <0.01 | <0.01 | <0.01 | <0.01 | <0.01 | <0.01 | <0.01 | <0.01 | <0.01 | <0.01 | <0.01 | <0.01 | <0.01 | <0.01 | <0.01 | <0.01 | <0.01 |
| CaO | 11.30 | 18.30 | 5.05 | 0.455 | 0.03 | 3.55 | 5.33 | 2.29 | 2.48 | 6.00 | 6.61 | 7.07 | 0.13 | 6.80 | 1.61 | 2.39 | 1.52 | 8.14 | 4.95 |
| $K_2O$ | <0.01 | <0.01 | <0.01 | <0.01 | <0.01 | 0.15 | <0.01 | <0.01 | <0.01 | <0.01 | <0.01 | <0.01 | <0.01 | <0.01 | <0.01 | <0.01 | 0.195 | <0.01 | 0.03 |
| $Na_2O$ | <0.01 | <0.01 | <0.01 | <0.01 | <0.01 | <0.01 | <0.01 | <0.01 | <0.01 | <0.01 | <0.01 | <0.01 | <0.01 | <0.01 | <0.01 | <0.01 | <0.01 | <0.01 | <0.01 |
| $P_2O_5$ | 0.94 | 0.83 | 0.898 | 0.96 | 0.97 | 1.04 | 0.94 | 1.05 | 0.93 | 0.88 | 0.90 | 0.91 | 1.03 | 0.95 | 0.96 | 0.84 | 0.99 | 0.83 | 0.94 |
| $TiO_2$ | <0.01 | <0.01 | <0.01 | <0.01 | <0.01 | <0.01 | <0.01 | <0.01 | <0.01 | <0.01 | <0.01 | <0.01 | <0.01 | <0.01 | <0.01 | <0.01 | <0.01 | <0.01 | <0.01 |
| **Total** | 90.55 | 90.62 | 88.38 | 87.78 | 88.40 | 89.25 | 88.70 | 88.79 | 89.71 | 89.50 | 88.58 | 88.76 | 88.53 | 88.69 | 87.39 | 88.39 | 89.06 | 88.66 | 88.87 |

DOI: 10.56892/bima.v8i4.1152

**Table 2: Trace Elements concentration of mineralized baryte veins from the area of study (all values are in ppm)**

| Trace Elements (ppm) | Baryte separate | | | | | | | | | | | | | | | | | |
|---|---|---|---|---|---|---|---|---|---|---|---|---|---|---|---|---|---|---|
| | Gombe Baryte | | | | | | | | | Liji Baryte | | | | | | | | |
| | SB1 | SB2 | SB3 | SB4 | SB5 | SB6 | SB7 | SB8 | SB9 | SB10 | SB11 | SB12 | SB13 | SB14 | SB15 | SB16 | SB17 | SB18 |
| Ba | 513000 | 599000 | 735000 | 758000 | 770000 | 712000 | 740000 | 755000 | 780000 | 743000 | 746000 | 742000 | 767000 | 728000 | 770000 | 787000 | 740000 | 730000 |
| Sr | 14100 | 17700 | 23300 | 27000 | 25100 | 18700 | 17800 | 15900 | 15900 | 20400 | 21700 | 21200 | 17000 | 18600 | 28600 | 28900 | 21100 | 24600 |
| Cl | 355.00 | 447.00 | 427.00 | 388.00 | 387.00 | 376.00 | 348.00 | 346.00 | 315.00 | 395.00 | 379.00 | 374.00 | 400.00 | 445.00 | 401.00 | 362.00 | 373.00 | 393.00 |
| S | 58700 | 68100 | 86900 | 91200 | 87500 | 80700 | 83200 | 82900 | 81300 | 80500 | 86000 | 82800 | 87500 | 82500 | 90800 | 88900 | 84500 | 84000 |
| V | 9030 | 14300 | 14300 | 14200 | 12500 | 12100 | 14400 | 12300 | 8550 | 11500 | 13800 | 14600 | 11900 | 15100 | 16800 | 12100 | 11600 | 14700 |
| Ni | <0.01 | <0.01 | <0.01 | <0.01 | <0.01 | <0.01 | <0.01 | <0.01 | <0.01 | <0.01 | <0.01 | <0.01 | <0.01 | <0.01 | 52.80 | 28.70 | <0.01 | 34.70 |
| Cu | <0.01 | 19.80 | 171.0 | 122.0 | <0.01 | 23.50 | 25.30 | 29.00 | <0.01 | <0.01 | <0.01 | 20.00 | 12.20 | 18.50 | 139.0 | 119.0 | 57.90 | 135.0 |
| Zn | <0.01 | <0.01 | 31.10 | <0.01 | <0.01 | <0.01 | <0.01 | <0.01 | <0.01 | <0.01 | <0.01 | <0.01 | <0.01 | <0.01 | <0.01 | <0.01 | <0.01 | 25.40 |
| Y | 71.10 | 33.80 | <0.01 | <0.01 | <0.01 | 29.30 | 27.00 | <0.01 | <0.01 | <0.01 | 30.80 | 28.80 | <0.01 | 39.60 | <0.01 | <0.01 | 38.60 | 82.90 |
| Zr | 419.0 | 969 | 1250 | 1420 | 1350 | 965 | 952 | 837 | 986 | 1170 | 1180 | 1150 | 889 | 938 | 1440 | 1810 | 1250 | 1330 |
| Ta | <0.01 | <0.01 | <0.01 | 131.0 | <0.01 | <0.01 | <0.01 | <0.01 | <0.01 | <0.01 | <0.01 | <0.01 | <0.01 | <0.01 | 181.00 | 192.00 | <0.01 | 184.00 |
| Pb | <0.01 | <0.01 | <0.01 | 45.70 | <0.01 | <0.01 | <0.01 | <0.01 | <0.01 | <0.01 | <0.01 | <0.01 | <0.01 | <0.01 | <0.01 | <0.01 | <0.01 | <0.01 |
| Zn | <0.01 | <0.01 | 31.10 | <0.01 | <0.01 | <0.01 | <0.01 | <0.01 | <0.01 | <0.01 | <0.01 | <0.01 | <0.01 | <0.01 | <0.01 | <0.01 | <0.01 | 25.40 |
| As | 31.60 | <0.01 | <0.01 | 20.60 | <0.01 | <0.01 | <0.01 | <0.01 | <0.01 | <0.01 | <0.01 | <0.01 | <0.01 | <0.01 | <0.01 | <0.01 | <0.01 | <0.01 |
| Rb | <0.01 | <0.01 | <0.01 | <0.01 | <0.01 | <0.01 | <0.01 | <0.01 | <0.01 | <0.01 | <0.01 | <0.01 | <0.01 | <0.01 | <0.01 | <0.01 | 59.10 | <0.01 |
| Br/Sr | 36.38 | 33.84 | 31.55 | 28.07 | 30.68 | 38.07 | 41.57 | 47.48 | 49.06 | 36.42 | 34.38 | 35.00 | 45.12 | 39.14 | 26.92 | 27.23 | 35.07 | 29.67 |
| | **Rare Earth Elements** | | | | | | | | | | | | | | | | | |
| Eu | 1.78 | 1.25 | <0.01 | <0.01 | <0.01 | <0.01 | <0.01 | <0.01 | 3.01 | <0.01 | <0.01 | <0.01 | <0.01 | <0.01 | <0.01 | <0.01 | <0.01 | <0.01 |
| Gd | <0.01 | 2.38 | <0.01 | <0.01 | <0.01 | 1.90 | 2.56. | <0.01 | 3.62 | 2.20 | <0.01 | <0.01 | <0.01 | 2.81 | <0.01 | 2.09 | 2.06 | <0.01 |
| Tb | 7.45 | 4.80 | 2.57 | 3.24 | 3.99 | 4.83 | 5.11 | 4.29 | 3.74 | 3.71 | 4.68 | 4.55 | 4.40 | 5.39 | 2.78 | 4.77 | 4.97 | 4.91 |
| Dy | 1.78 | 2.09.0 | 2.30 | 2.77 | 2.43 | 2.04 | 2.09 | 1.93 | 2.54 | 2.30 | 2.06 | 2.36 | 2.07 | 2.05 | 2.57 | 3.16 | 2.74 | 2.78 |
| Nd | 4.55 | 6.07 | 8.17 | 8.93 | 7.55 | 8.99 | 9.56 | 1.00 | 5.92 | 7.32 | 8.31 | 9.16 | 10.00 | 10.00 | 10.80 | 5.12 | 6.32 | 7.55 |
| **ΣLREE** | 6.28 | 9.70 | 8.17 | 8.93 | 7.55 | 10.89 | 12.12 | 1.00 | 12.55 | 9.52 | 8.31 | 9.16 | 10.00 | 12.81 | 10.80 | 7.21 | 8.38 | 7.55 |
| **ΣHREE** | 9.23 | 6.89 | 4.87 | 6.01 | 6.42 | 6.87 | 7.20 | 6.22 | 6.28 | 6.01 | 6.74 | 6.91 | 6.47 | 7.44 | 5.35 | 7.93 | 7.71 | 7.69 |
| **ΣREE** | 15.51 | 16.59 | 13.04 | 14.94 | 13.97 | 17.76 | 19.32 | 7.22 | 18.83 | 15.53 | 15.05 | 16.07 | 16.47 | 20.25 | 16.15 | 15.14 | 16.09 | 15.24 |

DOI: 10.56892/bima.v8i4.1152

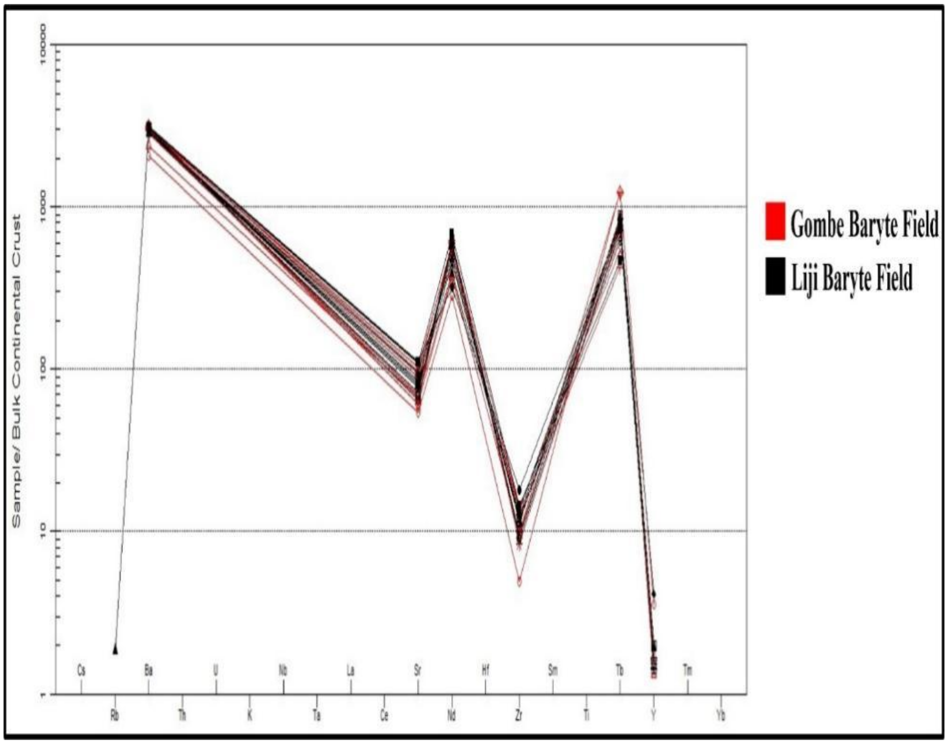

**Figure 3:** Multi-element variation diagram illustrating geochemical characteristics of baryte mineralization from the study area (chondrite normalizing values, Taylor and McLennan, 1985).

## DISCUSSION

### Differentiations Index of Barium Metals

The plot of BaO against $SiO_2$, SrO, CaO, $Fe_2O_3$, $P_2O_5$, $Al_2O_3$, and S serves as an index of differentiation (Figure 4). This plot indicates a positive correlation between BaO and both SrO and S, while showing a negative correlation with $SiO_2$ and CaO. $Fe_2O_3$ exhibits both positive and negative correlations with BaO. $Al_2O_3$ and $P_2O_5$ do not display any correlation (Figure 4). A strong positive correlation is expected between BaO, SrO, and S, indicating a shared association in mineral formation. The significant negative correlation between BaO and CaO suggests that barium and calcium minerals may have competed for available sulfate ions ($SO_4^{2-}$) in oxidized environments due to their similar ionic radii. However, because calcium is more reactive than barium, it preferentially combined with sulfate ions to form anhydrite, since oxidizing conditions stabilize sulfate ($SO_4^{2-}$), encouraging anhydrite formation. This process allowed barium to crystallize a pure baryte in the study area. The varying trends of $Fe_2O_3$ may reflect the early and late crystallization of iron oxides (Figure 4).

The concentrations of BaO and SrO in the Gombe baryte field are lower compared to those in the Liji baryte field and show an inverse relationship with $SiO_2$ concentration. However, the concentrations of BaO and SrO increase with depth, indicating that the quality of the baryte ores in both Gombe and Liji fields is depth-dependent. Additionally, $Al_2O_3$ and $TiO_2$ concentrations in the baryte veins are very low for both fields, which is characteristic of major ores formed through hydrothermal processes (Lottermoser & Ashley, 1996).

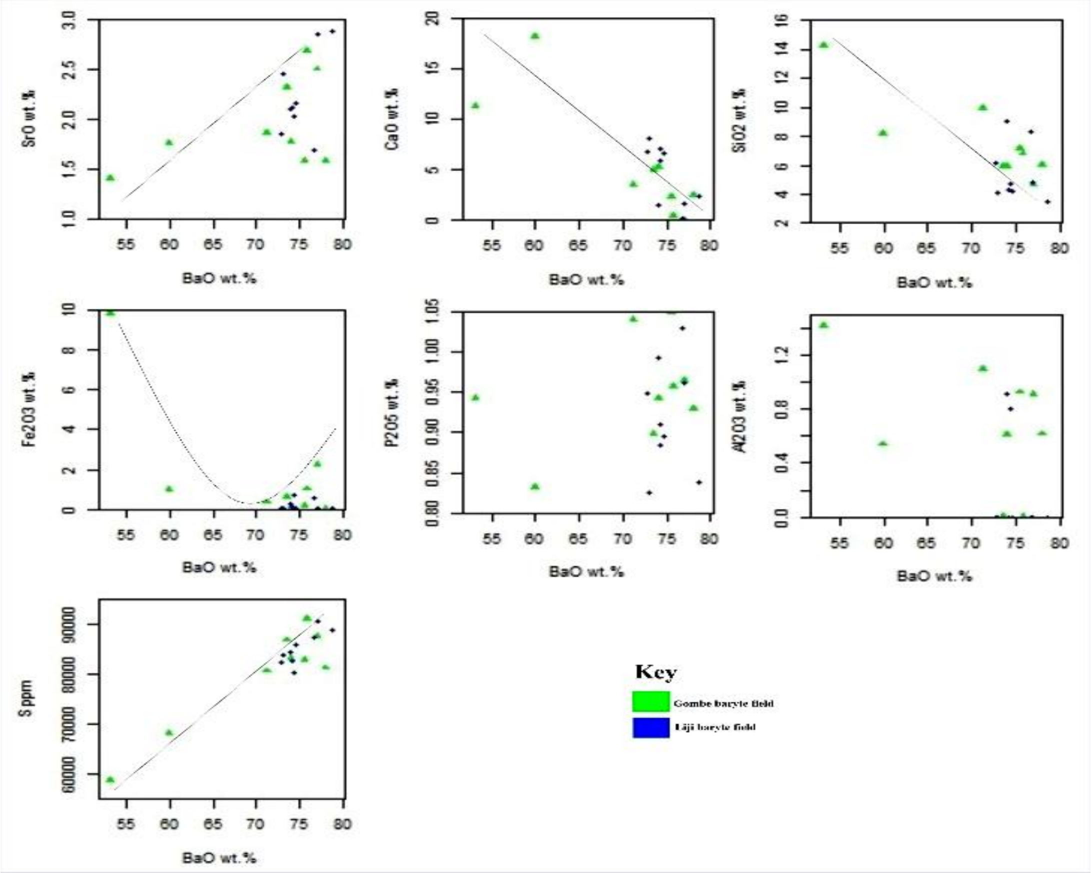

**Figure 4:** Bivariate plot of BaO versus SrO, $SiO_2$, CaO, $Al_2O_3$, $P_2O_5$, $F_2O_3$ (wt. %) and S in ppm of baryte samples from the study area.

## Provenance Indicators and Implication for Fluid Mixing

Mixing diagrams that incorporate the elements Al, Mn, Fe, and Ti have been successfully used to illustrate the mixing ratios of hydrothermal and pelagic components of barium metals in ancient sedimentary basins (Pinto-Auso and Harper 1985). The logarithm of Ba concentration for all baryte samples from the Gombe and Liji fields was plotted against the concentration ratio of Al/(Al+Fe+Mn). A ratio of Al/(Al+Fe+Mn) > 0.50 typically indicates pelagic sediments, while a ratio < 0.35 points to a substantial contribution from hydrothermal sources (Bostrom and Peterson, 1969). Most samples from the study area exhibit ratios of Al/(Al+Fe+Mn) < 0.35, although a few exceed 0.50. This indicates that barium in the area comes from two main sources: hydrothermal inputs and the surrounding rocks. However, the hydrothermal contribution to baryte mineralization is much greater than the barium extracted from the surrounding rocks by invading hydrothermal fluids (Figure 5). Therefore, it can be concluded that the barium-rich fluids predominantly originate from magmatic hydrothermal sources. These fluids likely became enriched with barium by leaching it from oceanic and/or continental rocks.

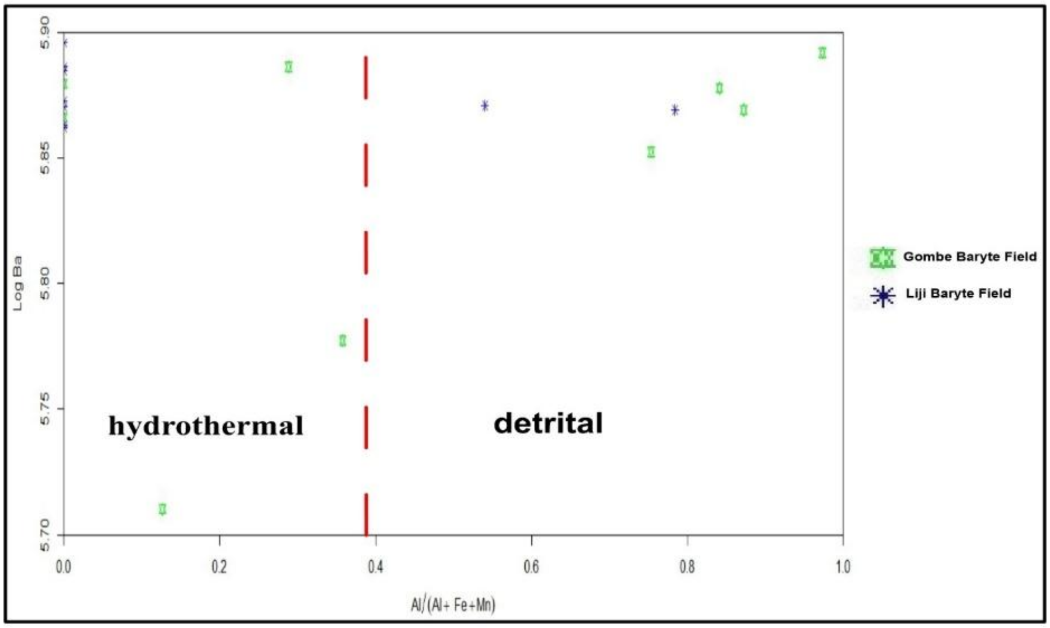

**Figure 5:** Plots of Al/(Al+Fe+Mn) metal ratios versus Log (Ba). All concentrations are in ppm (Paul and robert, 1991).

## Markers for Redox Conditions of Barytes Precipitation

Studies of trace and rare earth elements (REE) can be employed to ascertain the physico-chemical conditions and the sources of mineralized fluids across various geological environments (Jurkovic et al., 2010; Noguchi et al., 2011). The trace elements Cu, Pb, Zn, and Fe (present as hematite) detected in several analyzed samples provide valuable insights into the redox conditions during the formation of baryte crystals. The occurrence of lead, zinc, copper and iron in some baryte samples from the Gombe inlier suggests that the mineralization process primarily occurred under reducing conditions. However, the presence of iron oxides in certain samples points to localized episodes of more oxidizing environments. Iron might have been present as pyrite ($FeS_2$ ) or other reduced forms. Later exposure to oxygen (e.g., due to upliftment) could oxidize the iron, forming iron oxides.

Another indicator of redox conditions is the europium (Eu) anomaly. The behavior of Eu in a mineralized system is sensitive to temperature, as it can be depleted in low-temperature environments or enriched in high-temperature conditions (Vaslsami and Cann, 1992; Bau, 1991). The positive Eu anomalies observed in the Gombe baryte field (Figure 6) suggest that these baryte samples were deposited from hydrothermal fluids in a relatively reducing environment (Guichard et al., 1979; Barrett et al., 1990). In contrast, the negative Eu anomalies detected in the Liji baryte field (Figure 6) indicate that late-stage mineralization occurred in a shallow and oxygenated environments under low-temperature conditions. Thus, the fluctuations between positive and negative Eu anomalies in the Gombe and Liji baryte fields suggest that the mixing of Ba-bearing hydrothermal fluids and sulfur-rich seawater in the study area occurred under varying reducing - oxidizing conditions in low-temperature or near-surface environments, as evidenced by the inconsistent nature of the Eu anomalies.

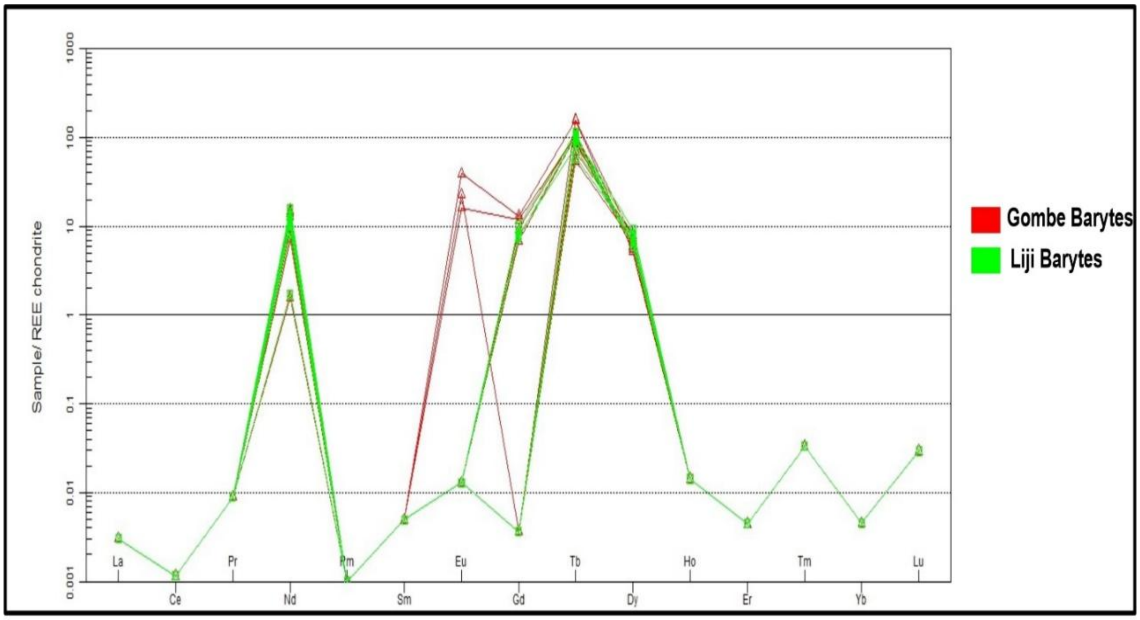

**Figure 6:** Chondrite-normalized REE patterns of baryte mineralization from Gombe and Liji fields. Normalizing values were those of Nakamura, (1974).

### Comparison of the Gombe-Liji Baryte Deposits with other Baryte Occurrences in the Benue Trough and the World at Large

To determine the likely origin of the Gombe-Liji baryte deposit, the average rare earth element (REE) profiles of the samples were normalized according to Nakamura (1974) and compared with those from various baryte deposits worldwide (Figure 7 and Table 3). This comparison included: (a) pelagic baryte from the central Pacific (Michard & Albarede, 1986), deeply buried (diagenetic) baryte from the northeast Pacific (Michard & Albarede, 1986), hydrothermal vein baryte from Sterling, Colorado, USA (Michard, 1989), and seawater-dominated hydrothermal fluids (Boynton, 1984); (b) baryte mineralization from the Gaidam and Wuyaku regions in the Northern Benue Trough (El-Nafaty, 2017); and (c) baryte deposits from the Lessel-Ihugh area in the Southern Benue Trough (Ngukposu, 2015) (Table 3). The distribution patterns of REEs in baryte occurrences from parts of the Benue Trough and globally were analyzed to infer the potential origins and formation environments of barytes, as suggested by Bozkaya and Gokce (2004).

The comparison of average rare earth element (REE) patterns among various baryte deposits, including the Gombe and Liji deposits, reveals generally low concentrations of REEs across all samples, with the exceptions of La and Ce anomalies in pelagic (MB9) and hydrothermal (CB3) vein barytes, which exceed 100 ppm (Table 3). The chondrite-normalized REE profiles of the baryte mineralization in the study area align closely with those of other occurrences in the Benue Trough. The Gaidam and Wuyaku barytes from the Northern Benue Trough show similar patterns, exhibiting both positive and negative anomalies for Eu and Gd. In contrast, the Lessel-Ihugh barytes from the Southern Benue Trough display positive Gd and negative Eu anomalies (Figure 7). This suggests a temperature variation between the Gombe-Liji barytes and the Lessel-Ihugh barytes, while similar precipitation conditions likely existed for the Gombe-Liji, Gaidam, and Wuyaku deposits, which formed under low to medium temperature conditions. The differences in elevation, with the higher Gombe inlier and parts of the Northern Benue Trough compared to the lower Southern Benue Trough, may have influenced the temperature variations during baryte precipitation in the region.

**Table 3:** Comparison of REEs from Gombe and Liji baryte, with contents of various baryte occurrences and hydrothermal systems in some part of the Benue Trough and the World.

| Rare Earth Elements | Baryte mineralization in the Benue Trough | | | | Baryte mineralization in the World | | | |
|---|---|---|---|---|---|---|---|---|
| (ppm) | G-LB | LBM[c] | GBM[b] | WBM[b] | MB2[a] | MB9[a] | CB3[a] | Seawater[a] |
| La | - | 5.4 | 6.45 | 7.05 | 13 | 143.0 | 75 | 3.1 |
| Ce | - | 6.3 | 8.9 | 6.7 | 3.5 | 309.0 | 103 | 1.2 |
| Pr | - | 0.14 | 0.87 | 0.68 | - | 12.50 | - | 0.64 |
| Nd | 7.52 | 1.56 | 3.5 | 2.8 | - | - | - | 2.5 |
| Sm | - | 0.38 | 1.1 | 0.95 | 0.38 | 7.40 | 0.98 | 0.43 |
| Eu | 2.01 | 0.02 | 0.78 | 2.11 | 0.1 | 1.70 | 0.45 | 0.12 |
| Gd | 2.45 | 3.37 | 0.85 | 0.95 | - | - | - | 0.65 |
| Tb | 4.45 | 0.09 | 0.1 | 0.1 | - | - | - | 0.14 |
| Dy | 2.34 | 0.05 | 0.35 | 0.4 | 0.54 | 14.0 | 1.00 | 0.82 |
| Ho | - | 0.04 | - | - | 0.18 | 5.70 | - | 0.22 |
| Er | - | 0.12 | 0.1 | 0.2 | - | 1.80 | - | 0.68 |
| Tm | - | 0.04 | - | - | - | - | - | 0.15 |
| Yb | - | 0.27 | 0.1 | 0.2 | - | 26.0 | - | 0.63 |
| Lu | - | 0.02 | - | 0.4 | - | - | - | 0.17 |

**References**

(a) (Guichard et al.1979)

(b) (El-Nafaty, 2017)

(c) (Labe, 2015)

**Baryte Samples**

**G-LB:** Average baryte Northern Benue Trough (this study)
**GBM[b]:** Gaidam barytes Northern Benue Trough
**WBM[b]:** Wuyaku baryte Northern Benue Trough
**LBM[c]**: barytes in Lessel-Ihugh area Southern Benue Trough
**MB2[a]:** pelagic baryte (central Pacific) (Michard & Albarede, 1986)
**MB9[a]:** deeply buried (diagenetic) baryte (northeast Pacific) (Michard & Albarede, 1986)
**CB3[a]:** hydrothermal vein baryte (Sterling, Colorado, USA) (Michard, 1989)
**Seawater[a]** - Seawater dominated hydrothermal fluid (Boynton, 1984)

The average REE profiles of the Gombe-Liji baryte samples reveal distinct distribution patterns when compared to various types of barytes found worldwide (Figure 7). Specifically, seawater, MB2, MB9, and CB3 barytes correspond to seawater-dominated hydrothermal fluids, pelagic deposits, deeply buried (diagenetic) barytes, and hydrothermal

DOI: 10.56892/bima.v8i4.1152

vein barytes, respectively. The REE profiles of the study area's baryte samples closely resemble those of seawater-dominated hydrothermal profiles, both exhibiting negative anomalies for Ce, Dy, and Gd, and positive anomalies for Tb. In contrast, the hydrothermal vein baryte from Colorado (CB3) shows a similar profile to that of the Gombe-Liji barytes, particularly characterized by positive Eu anomalies. This resemblance suggests that the baryte mineralization in the Gombe-Liji area was likely deposited by seawater-bearing hydrothermal fluids.

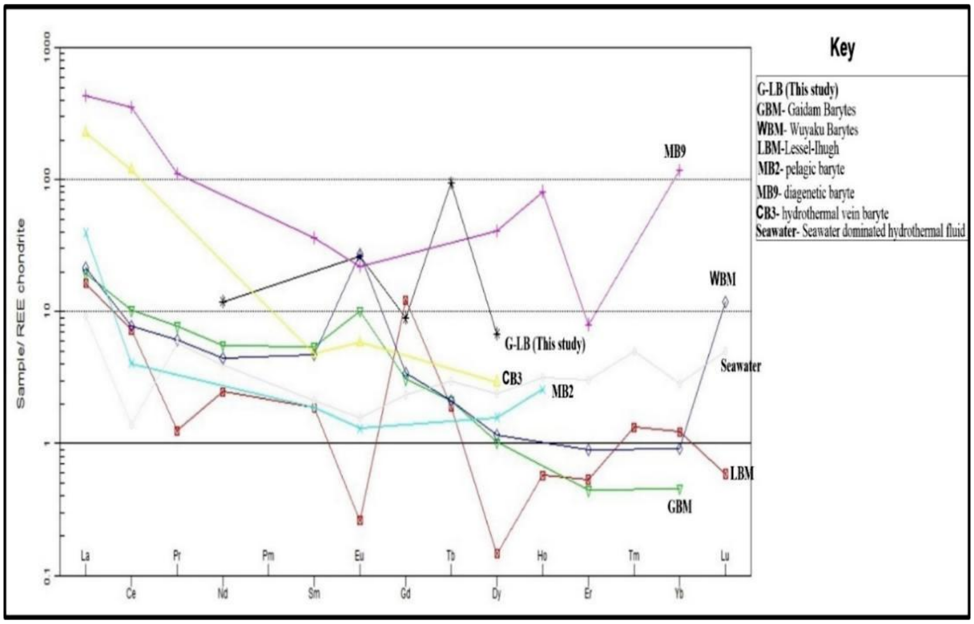

**Figure 7:** Comparison of the rare-earth element distributions pattern of baryte in the study area with other occurrences in some part of Benue Trough and some part of the world.

## CONCLUSION

The geochemical analysis of baryte mineralization in the Gombe Inlier provides significant insights into its origin, formation conditions, and crystallization environment. The study indicates that the mineralizing fluid was a highly differentiated hydrothermal fluid, enriched in barium (Ba) and strontium (Sr) but depleted in high field strength elements (e.g., Hf, Zr, Ta, Nb, and rare earth elements [REEs]), which precipitated earlier during the mineralization process. Late-stage fluids concentrated incompatible elements like Ba and Sr, suggesting the baryte deposits in the Gombe Inlier represent the baryte end-member of the baryte-celestine solid solution series.

These Ba-rich fluids are derived from magmatic hydrothermal sources (juvenile water) and incorporate additional barium from oceanic or continental rocks, or a mixture of both. The presence of trace elements such as Cu, Pb, Zn, and iron oxides, along with variable europium (Eu) anomalies across baryte fields, supports the hypothesis that baryte precipitated from seawater-bearing hydrothermal fluids under fluctuating oxic-anoxic conditions in low-temperature or near-surface settings.

Comparative analyses reveal that the baryte deposits of the Gombe Inlier share characteristics with other regional and global occurrences, consistent with formation in low- to medium-temperature environments typical

DOI: 10.56892/bima.v8i4.1152

of seawater-influenced hydrothermal systems. Additionally, elevation differences between the Southern and Northern Benue Troughs appear to have influenced variations in redox conditions associated with baryte mineralization in the Benue Trough.

## REFERENCES

Auwalu D., Haruna A. I., Maigari A. S., Bata T. P., Abubakar U., Yusuf A. and Sulaiman A. (2024). The Structural Attributes of Gombe Lineaments in relation to Baryte-Fluorite mineralization in the Gongola Sub-basin of the Northern Benue Trough, Nigeria: A Study Using Remote Sensing Data. Bima Journal of Science and Technology, Vol. 8(1B) Apr, 2024 ISSN: 2536-6041

Barrett, T.J., Jarvis, I. and Jarvys, K.E. (1990). Rare earth element geochemistry of massive sulfides-sulfates and gossans on the Southern Explorer Ridge. *Geology* 18, 583–586.

Bau, M. (1991). Rare-earth element mobility during hydrothermal and metamorphic fluid rock interaction and the significance of the oxidation state of europium. Chemical Geology, 93, 219-230.

Benkhelil, J. (1989). The origin and evolution of the cretaceous Benue Trough. Nigeria Jous of African Earth Sciences, pp. 225 – 282.

Bostrom, K., and Peterson, M. N.A. (1969). Origin of aluminum poor ferro-magnesiu sediments in areas of high heat flow on the East Pacific Rise: Mar. Geol.,v. 7, p. 427-447.

Boynton, W.V. (1984). Geochemistry of the rare earth elements: meteorite studies. In: HENDERSON, P. (ed), Rare Earth Element Geochemistry, Elsevier, 63—114.

Byemi J., Zaborski P.M., Anyiam O.A., and Nzekwe E.I. (2015). Field Study of the Positive Flower Structures of the Gombe Inlier, Upper Benue Trough, Northeastern Nigeria. Journal Geological Society of India Vol.85, February 2015, pp.183-196.

Bozkaya, G. and Gokce, A. (2004). Trace and Rare-Earth Element Geochemistry of the Karalar (Gazipasa-Antalya) baryte-galena deposits, Southern Turkey. Turkish Journal of Earth Sciences, 13, 63-76.

Cathles L. M. (1997). Thermal aspects of ore formation. *In* Geochemistry of Hydrothermal Ore Deposits ($3^{rd}$ Edn) HL Barnes (Ed) Wiley, New York, p 191-228

Clark, H.B, Poole, F.G. and Wang, Z. (2004). Comparison of some sediment hosted, stratiform barite deposits in China, the United States, and India. *Ore Geology Reviews* 24, 85–101.

Croffie, M.E., Williams, P.N., Fenton, O., Fenelon, A., Metzger, K., and Daly, K. (2020). Optimising sample preparation and calibrations in EDXRF for quantitative soil analysis. Agronomy 10, 1309.

El-Nafaty, J.M. (2017). Rare earth element and stable sulphur (*d* 34S) isotope study of Barite – copper mineralization in Gulani area, Upper Benue Trough, NE Nigeria. Journal of African Earth Sciences p. 154-156.

Garven G., and Raffensperger J. P. (1997). Hydrogeology and geochemistry of ore genesis in sedimentary basins. *In* Geochemistry of Hydrothermal Ore Deposits, 3rd edn. HL Barnes (Ed) Wiley, New York, p 797- 875s.

Grant, N.K. (1971). South Atlantic, Benue Trough and Gulf of Guinea Cretaceous triple junction. Bulletin Geological Society of America, 82, 2295-2298.

Guichard, F., Church, T., Treuil, M. and Jaffrezic, H. (1979). Rare earths in barytes: distribution and effects on

DOI: 10.56892/bima.v8i4.1152

aqueous partitioning. *Geochimica et Cosmochimica Acta,* 43, 983-997

Guiraud M. (1993). Late Jurassic rifting - Early Cretaceous rifting anf late Cretaceous transpressional inversion in the upper Benue Basin (NE- Nigeria) Bull centers Rech.Explor-prod.Elf. Aquitaine, 17, 371-383.

Guiraud, R., Maurin, J. C. (1992). Early cretaceous rifts of western and central africa: an overview. Tectonophysics 213, 153–168.

Guiraud, M. (1990). Mecanisine de formation du basin cretacesurdecroachment multiple de la Hante Benue (Nigeria) facieset geometric des corps sedimentaires – mem. Habilitation, univ. Montpellier 445pp.

Hanor, J.S. (2000). Baryte - celestine geochemistry and environments of formation. In: Reviews in Mineralogy & Geochemistry – Sulfate Minerals (Eds C.N. Alpers, J.L. Jambor and D.K. Nordstrom), 40, pp. 193–275. Mineralogical Society of America, Washington, D.C.

Haruna, A.I. (2007). Geology and Economic potential of baryte mineralization in Gombe Inlier, Gombe State Nigeria. pp 1-4.

Jamieson, J. W., Hannington, M. D., Tivey, M. K., Hansteen, T., Williamson, N. M. B., Stewart, M., Fietzke, J., Butterfield, D., Frische, M., Allen, L., Cousens, B., and Langer, J. (2016). Precipitation and growth of barite within hydrothermal vent deposits from the endeavour segment, Juan de Fuca Ridge. *Geochimica et Cosmochimica Acta*, 173: 64-85.

Jewell, P.W and Stallard, R.F. (1991). Geochemistry and paleoceanographic setting of central Nevada bedded barites. *Journal of Geology* 99, 151–170.

Jurković, I., Garašić, V. and Hrvatović, H. (2010). Geochemical characteristics of barite occurrences in the Palaeozoic complex of south-eastern Bosnia and their relationship to the barite deposits of the mid-Bosnian Schist Mountain. *Geologia Croatica* 63, 241–258

Labe, N.L. (2015). Geochemical and Geotechnical characterization of baryte mineralization in Lessel and Ihugh areas, Lower Benue Trough, Nigeria. Unpublished M.Sc. thesis. pp. 97- 13.

Lottermoser, B.G. and Ashley, P.M. (1996). Geochemistry and exploration significance of ironstones and barite-rich rocks in the Proterozoic Willyama Supergroup, Olary Block, South Australia. *Journal of Geochemical Exploration* 57, 57–73.

Michard, A. (1989). Rare earth element systematics in hydrothermal fluids. *Geochimica et Cosmochimica Acta, 53, 745-750.*

Michard, A. and Albarade, F. (1986). The REE content of some hydrothermal fluids. *Chemical Geology,* 55, 51-60.

Ministry of Mines and Steel Development. Barytes Exploration Opportunities in Nigeria, (2010). pp. 1 – 7.

Nakamura, N. (1974). Determination of REE, Ba, Fe, Mg, Na and K in carbonaceous and ordinary chondrites. Geochim Cosmochim Acta, 38, 757-775.

Noguchi, T., Shinjo, R., Ito, M., Takada, J. and Oomori, T. (2011). Baryte geochemistry from hydrothermal chimneys of the Okinawa Trough: insight into chimney formation and fluid/sediment interaction.J. Mineral.Petrol. Sci., 106, 26-35.

Nwajide, C. (2013). Geology of Nigeria's Sedimentary Basins. CSS Bookshop Limited. Olade, M.A. (1975). Evolution of Nigeria‟s Benue Trough (aulacogen).

DOI: 10.56892/bima.v8i4.1152

A tectonic model. Geological Magazine, 112, 575-583.

Paul W. J and Robert F. S. (1991). Geochemistry and Paleoceanographic Setting of Central Nevada Bedded Barites. The Journal of Geology, Vol. 99, No. 2 (Mar., 1991), pp. 151-170.

Pinto-Auso, M., and Harper, G. D. (1985). Sedimentation, metallogenesis, and tectonic origin of the basal Galice Formation overlying the Josephine ophiolite, northwestern California: Jour. Geol., v. 93, p. 713-725.

Rabiu, M., Ahmed, I. H., and Buhari, S. (2019). The structural control of barite mineralization in Gombe inlier within Gongola basin Upper Benue Trough, Nigeria. International Journal of Environmental Studies and Safety Research ISSNISSN: 25362536-7277 (Print): 2536-7285 (Online) Volume 4, Number 4, pp 42-56.

Rousseau, R. (2013). How to apply the fundamental parameters method to the quantitative X-ray fluorescence analysis of geological materials. Journal of Geosciences and Geomatics 1, 1–7.

Stoneley, R. (1966). The Niger Delta region in the light of the theory of continental drift. Geol. Mag. 103, 385–397.

Taylor, S.R. and McLennan, S.M. (1995). The geochemical evolution of the continental crust. Reviews in Geophysics, 33, 241-625.

Tijani M. N, Loehnert E. P (2004) Exploitation and traditional processing techniques of brine salt in parts of the Benue Trough, Nigeria. Int J Miner Process 74:157–167.

Vaslsami, E. and Cann, J.R. (1992). Mobility of rare earth elements in the zones of intense hydrothermal alteration in the Pindos ophiolite, Greece. In: Parson, L.M., Murton, B.J. and Browning, P., eds., *Ophiolites and their modern oceanic analogues*, Geological SocietySpecial Publication, 60, 219-232.

Zaborski P.M. (1998). A Review of the Cretaceous System in Nigeria.Afri.Geo.Rev; 5, 385-483.

Zaborski, P.M. (2003) Guide to the Cretaceous systems in the upper part of the Benue Trough, northeastern, Nigeria. Afri. Geosci. Rev. v.10(1&2), pp.13-32.